

Ferredoxin NADP+ reductase for NADPH and NADH regeneration in a flow bioelectrochemical reactor

Wassim El Housseini, François Lapicque, Alain Walcarius, Elisabeth Lojou, Nicolas Rouhier, Mathieu Etienne

▶ **To cite this version:**

Wassim El Housseini, François Lapicque, Alain Walcarius, Elisabeth Lojou, Nicolas Rouhier, et al.. Ferredoxin NADP+ reductase for NADPH and NADH regeneration in a flow bioelectrochemical reactor. Bioelectrochemistry, 2025, 164, pp.108919. ⟨10.1016/j.bioelechem.2025.108919⟩. ⟨hal-05099739⟩

HAL Id: hal-05099739

https://hal.inrae.fr/hal-05099739v1

Submitted on 5 Jun 2025

HAL is a multi-disciplinary open access archive for the deposit and dissemination of scientific research documents, whether they are published or not. The documents may come from teaching and research institutions in France or abroad, or from public or private research centers.

L'archive ouverte pluridisciplinaire **HAL**, est destinée au dépôt et à la diffusion de documents scientifiques de niveau recherche, publiés ou non, émanant des établissements d'enseignement et de recherche français ou étrangers, des laboratoires publics ou privés.



Distributed under a Creative Commons CC BY 4.0 - Attribution - International License

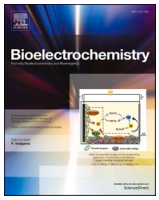
Bioelectrochemistry 164 (2025) 108919



Contents lists available at ScienceDirect

Bioelectrochemistry

journal homepage: www.journals.elsevier.com/bioelectrochemistry





Ferredoxin NADP$^+$ reductase for NADPH and NADH regeneration in a flow bioelectrochemical reactor☆

Wassim El Housseini [a,b], François Lapicque [b], Alain Walcarius [a], Elisabeth Lojou [c], Nicolas Rouhier [d], Mathieu Etienne [a,*]

[a] Université de Lorraine, CNRS, LCPME, F-54000 Nancy, France
[b] Université de Lorraine, CNRS, LRGP, F-54000 Nancy, France
[c] Aix Marseille Univ, CNRS, BIP, Bioénergétique et Ingénierie des Protéines, UMR 7281, 31, Chemin Joseph Aiguier CS 70071 13402 Marseille CEDEX 09, France
[d] Université de Lorraine, INRAE, IAM, F-54000 Nancy, France

ARTICLE INFO

Keywords:
Electroenzymatic regeneration
Ferredoxin-NADP$^+$ reductase
Flow reactor
Gas diffusion electrode
β-Nicotinamide adenine dinucleotide

ABSTRACT

Ferredoxin-NADP$^+$ reductase (FNR) is an efficient and selective biocatalyst to continuously regenerate the NADPH cofactor consumed in biomolecular synthesis for the chemical and pharmaceutical sectors. In this work, FNR from *Chlamydomonas reinhardtii* was applied to electrochemical regeneration of the nicotinamide cofactors, by combining this enzymatic catalyst in a flow reactor with the oxidation of hydrogen, a clean source of electrons and protons. FNR was immobilized on the surface of oxidized multi-walled carbon nanotubes, which allowed maintaining its activity for over six days under high flow rate. Surprisingly, this modified FNR electrode was effective not only in regenerating NADPH but also NADH. The cofactor regeneration was then applied to the NADH-dependent production of lactate from pyruvate, using L-lactate dehydrogenase (LDH) in the presence of low NAD$^+$ concentration (10 μM). Both FNR and LDH enzymes were immobilized in the bioelectrochemical system that achieved a remarkable total turnover number (TTN) of 10^4 for the nicotinamide cofactor and a faradaic efficiency higher than 80 %.

1. Introduction

Interfacing or mimicking natural systems is a very fertile research area [1,2]. For example, there is a huge interest in mimicking photosynthesis and mitochondria for regenerating NAD(P)H used in the conversion of CO_2 to pure chemicals [3–5]. Another exciting example is the development of bioinspired enzymatic systems that mimic the metabolic pathways in the human liver. These systems are designed to regenerate NAD(P)H efficiently, facilitating the biotransformation of drugs and detoxification processes [6,7]. By replicating the liver's natural ability to maintain redox balance and cofactor regeneration, these engineered enzymatic systems can significantly enhance the efficacy of therapeutic applications and biocatalysis in drug development. In this wide context, combining biology, electrochemistry, chemical engineering and flow chemistry appears a good pathway to reach efficient NAD(P)H cofactor applicable to biomolecular synthesis for the chemical and pharmaceutical sectors.

In bioelectrochemistry, the application of the regenerated form of the NADPH cofactor, or its oxidized form, includes a wide range of pure chemical production when coupled with a NADP-dependent enzyme [8]. The regeneration of the NADPH cofactor for biosynthesis of pure chemicals is a critical focus in bioelectrochemistry due to the cofactor's high cost. The stoichiometric addition of NADPH is not a viable option, necessitating the development of efficient regeneration methods to enable sustainable and economically-feasible chemical production.

Beyond the electrochemical regeneration of NADPH using electrochemical catalysts such as rhodium-based complexes [9,10], the electroenzymatic regeneration of this cofactor stands out as a crucial approach for achieving efficiency (high production rates) [11], selectivity (regeneration of 1,4-NADPH) [12], and sustainability in green chemistry. The electroenzymatic regeneration of the NADPH cofactor is primarily achieved by either NADPH diaphorase or ferredoxin-NADP$^+$ reductase (FNR) activities [13]. The primary difference between these catalysts is that NADPH diaphorase activity requires a redox mediator to act as an electron shuttle in a mediated electron transfer system (MET) for NADPH regeneration, as its electron transfer mechanism relies on

☆ This article is part of a special issue entitled: '11th SMCBS 2023 Workshop' published in Bioelectrochemistry.

* Corresponding author.
E-mail address: mathieu.etienne@cnrs.fr (M. Etienne).

https://doi.org/10.1016/j.bioelechem.2025.108919
Received 7 August 2024; Received in revised form 18 January 2025; Accepted 26 January 2025
Available online 27 January 2025
1567-5394/© 2025 The Authors. Published by Elsevier B.V. This is an open access article under the CC BY license (http://creativecommons.org/licenses/by/4.0/).

intermediaries to bridge the gap between the electrode and the enzyme's active site. In contrast, NADPH regeneration catalyzed by FNR can be achieved through both direct electron transfer (DET) and MET systems. The majority of studies reported in the literature focus on the electroenzymatic regeneration of NADPH catalyzed by FNR [12,14,15].

Remarkable progress has been made in developing immobilization methods for FNR in the context of NADPH regeneration [16]. Their wiring onto an electrochemical interface is achieved according to the two concepts as previously mentioned. The first one relies upon DET between the electrode and the biocatalyst immobilized on an electroactive surface such as indium-tin oxide electrode [17]. This method is advantageous because it ensures a more straightforward and efficient electron flow, reducing potential losses and enabling higher catalytic activity due to the close proximity of the electron donor and acceptor. Additionally, the direct electron transfer method often results in faster reaction rates and lower overpotentials, which are beneficial for energy-efficient processes [18]. The second one consists on MET using a redox mediator or a redox polymer that both can transfer electrons between the biocatalyst and the electrode [12,15]. The advantage of this method lies in its flexibility and adaptability. Redox mediators and polymers can facilitate electron transfer even when the biocatalyst and the electrode are not in direct contact, allowing for the use of a wider range of electrode materials and configurations. This method can also help to stabilize the biocatalyst, extend its operational lifetime, and improve the overall robustness of the electrochemical system by protecting the enzyme from direct interaction with potentially harmful electrode surfaces [19]. One of the criteria for the selection between both methods is the application requirements. The application of direct electron transfer between the electrode and the biocatalyst appears more suitable in a flow reactor [20].

Flow processes offer significant advantages over the conventional batch processes in biotechnology such as high mass transport and the improved production rate of the reactor allowed by applying high solution flow rates. Despite its inherent industrial concerns, translation of batch electrocatalysis to flow processes is more and more considered in industry. Unfortunately, the electroenzymatic regeneration of cofactors in a flow reactor represents a challenge with issues such as complex reactor design, insufficient stability of the immobilized catalyst, [21] and low conversion efficiencies [22]. Herein, our concern is to establish a flow bioelectrochemical reactor for the efficient electroenzymatic regeneration of the NAD(P)H cofactor catalyzed by FNR where the oxidation of hydrogen is the source of electrons and protons. Moreover, the integration of a gas diffusion electrode for hydrogen oxidation with an enzymatic bioelectrode was demonstrated to be a compelling strategy in reactors tailored for bioelectrochemical synthesis [23].

We previously described the efficiency of combining hydrogen oxidation and the regeneration of NAD(P)H electrochemically-catalyzed by a rhodium complex covalently immobilized on MWCNT in a flow reactor [24]. As enzymes provide higher selectivity and specificity, operating under mild, eco-friendly conditions, in the present work, the goal was to replace the rhodium complex by an electroenzymatic catalyst, FNR, immobilized on a carbon paper coated with oxidized MWCNT. After having developed the immobilization method and proved the activity of the system towards the regeneration of the NAD(P)H cofactor, a second enzyme has been immobilized on another CP-MWCNT for the biosynthesis of chemicals (Scheme 1). Among NAD(P)H-dependent dehydrogenases, L-lactate dehydrogenase (LDH) has been chosen for the bioconversion of pyruvate to lactate. The scheme of the whole arrangement is depicted in Scheme 1.

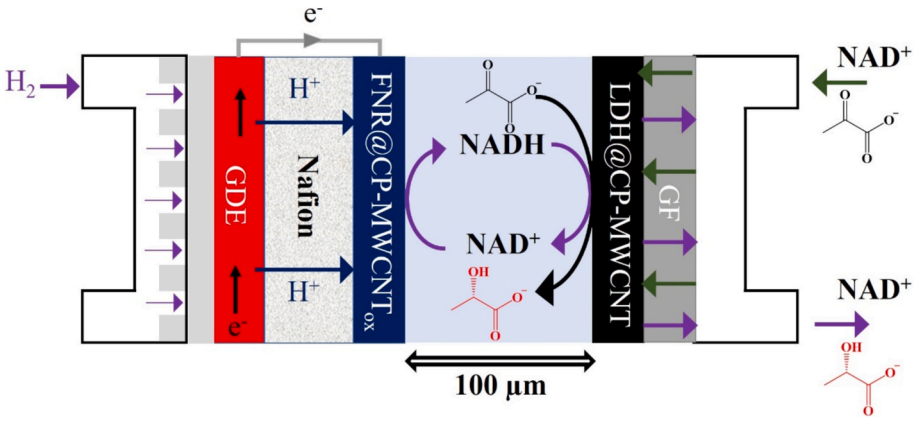
2. Materials and methods

2.1. Chemicals and reagents

β-nicotinamide adenine dinucleotide (NAD^+, >98 %), β-nicotinamide adenine dinucleotide phosphate ($NADP^+$, >98 %), [tris(hydroxymethyl)methylamino]propanesulfonic acid (TAPS, 97 %), L-lactate dehydrogenase (LDH) from rabbit muscle (≥ 600 units/mg protein), pyruvate (98 %), lactate (98 %) and H_2O_2 (98 %) were from Sigma-Aldrich. TAPS buffer (50 mM) was used to investigate the electrocatalytic properties of FNR towards $NAD(P)^+$ reduction and was reported to be one of the most appropriate for such experiments. Multiwalled carbon nanotubes (MWCNT, NC7000™ series) were from Nanocyl (Belgium). Gas diffusion electrodes (GDE), Nafion membrane (N-212), and carbon papers (SpectraCarb 2050L-0550 Carbon Paper) were acquired from Fuel Cell Store (USA). All solutions were prepared with high purity water (18 MΩ cm) from a Purelab Option water purification system.

2.2. Purification of recombinant FNR from Chlamydomonas reinhardtii

The sequence coding for the mature form (amino acids 27 to 346) of *Chlamydomonas reinhardtii* ferredoxin-$NADP^+$ reductase (FNR, Cre11.g476750) was cloned into the bacterial pET3d expression vector between NcoI and BamHI restriction sites using the following forward and reverse primers: 5′ cccccatgggccaccaaggcttcgacc 3′ and 5′ ccccggatcctagtagacctccacgtg 3′. The *E. coli* BL21(DE3) strain containing the helper pSBET plasmid was used for protein expression [25]. A culture of 2.4 L in lysogenic broth medium was performed at 37 °C supplemented with 50 μg/mL of kanamycin and ampicillin. Protein expression was induced at



Scheme 1. Schematic view of the flow electroenzymatic reactor. Solution flow is on the right side and hydrogen flow is on the left side. A proton-conducting Nafion membrane seperates the gas diffusion electrode, for hydrogen oxidation, from the FNR@CP-$MWCNT_{ox}$ electrode, for NADH production. On the top of FNR@CP-$MWCNT_{ox}$ electrode, LDH@CP-MWCNT was placed for the bioconversion of pyruvate to lactate catalyzed by LDH (NADH-dependent). The distance between both layers was approximately equal to 100 μm.

exponential phase by adding 100 μM of isopropyl β-D-1-thio-galactopyranoside during 4 h. Cells were harvested by centrifugation (Beckman Coulter JLA 8.1000; 20 min; 6,200 x g) and resuspended in 12 mL buffer A containing 30 mM Tris-HCl pH 8.0, 200 mM NaCl and 1 mM EDTA. Cell lysis was performed by sonication (20 % amplitude; 2 times 1 min), then soluble and insoluble fractions were separated by centrifugation (Beckman Coulter JA 25.50; 20 min; 48,000 x g; 4 °C). The soluble fraction was precipitated at 40 % of the ammonium sulfate saturation and then at 80 % in two successive steps separated by a centrifugation step (JA 25.50; 20 min; 30,800 x g; 4 °C). The 40–80 % precipitated fraction was resuspended in 8 mL buffer A and loaded on size exclusion chromatography (ACA 34, PALL Biosepra) equilibrated with buffer A. Fractions containing the protein of interest were pooled and dialyzed against buffer B containing 30 mM Tris-HCl pH 8.0 and 1 mM EDTA and loaded on Q-sepharose column (Cytiva). The non-retained protein fraction, containing FNR, was pooled and concentrated. Sample purity was assessed via SDS-PAGE and the concentration determined spectrophotometrically using theoretical molar extinction coefficients at 280 nm of 48735 $M^{-1}.cm^{-1}$ and at 455 nm of 8434 $M^{-1}.cm^{-1}$.

2.3. MWCNT oxidation with 30 % w/v H_2O_2

The oxidation of MWCNT followed a protocol reported in the literature [26]. 200 mg of MWCNTs were treated with 100 ml of a 30 % w/v H_2O_2 solution at 80 °C. In a round-bottom flask equipped with a condenser, thermocouple, and thermometer, the reaction was conducted. After stabilizing the temperature of the oil bath at 80 °C, the flask was immersed in the oil bath to initiate the oxidation process at a stirring rate of 200 rpm for 8 h. After oxidation, MWCNTs negatively charged were filtered and washed multiple times with distilled water until the pH of the filtered solution was neutral, and then dried overnight at 80 °C.

2.4. Preparation of CP-MWCNT$_{ox}$

The preparation of a 16 cm^2 CP-MWCNT or CP-MWCNTox was carried out as described in the method applied in a prior study [24]. A piece of SpectraCarb carbon paper (CP) (4 cm x 4 cm x 0.05 cm) was coated with MWCNT by sonicating 10 mg of MWCNT or MWCNT$_{ox}$ in a solution of ethanol (50 ml) for 5 h. This suspension was then vacuum-filtered onto the CP and allowed to dry overnight. This method ensures the effective deposition of MWCNT or MWCNT$_{ox}$ on the carbon paper, forming a stable and uniform layer suitable for the subsequent experimental steps.

2.5. Preparation of FNR@CP-MWCNT$_{ox}$ electrode

The immobilization of FNR was performed by being drop-casted on a 16 cm^2 CP-MWCNT$_{ox}$. Then, the electrode was left at a temperature of 2 °C until total adsorption of FNR.

2.6. Preparation of LDH@CP-MWCNT

The CP-MWCNT was prepared following a method used in a prior study [24]. LDH enzyme was adsorbed onto the surface of MWCNTs (16 cm^2) by depositing a 50 μl suspension of LDH and leaving it at 2 °C until total adsorption.

2.7. Electroenzymatic reactor

A 16 cm^2 gas diffusion electrode acted as the anode for hydrogen oxidation and a Nafion (N-212) membrane was inserted between the anode and the FNR@CP-MWCNT$_{ox}$ electrode for the separation of the two compartments while allowing migration of protons from the anode to the cathode (Scheme 1). In all tests in the electroenzymatic reactor, the hydrogen anode acts as a reference. In this study, the potential contribution of the ohmic drop to the measured potentials in the electrochemical system has not been explicitly quantified.

FNR@CP-MWCNT$_{ox}$ was stacked on a macroporous graphite felt in the cathodic chamber of the reactor. This felt facilitated a uniform distribution of the solution and ensured good electrical conduction with the graphite bipolar plate. In the absence of the enzymatic reaction, NAD(P)$^+$ entered the cathodic compartment, where it interacted with FNR (immobilized on the CP with oxidized MWCNT) and was reduced to NAD(P)H. The regenerated cofactor was then released from the reactor to a recipient, which was continuously degassed with N_2. The solution feeding to the flow reactor occurred in a loop between the reactor and the recipient. The detection of NAD(P)H was followed by UV absorption at 340 nm after suitable dilution ($A = \varepsilon lc$; $\varepsilon = 5.162\ mM^{-1}.cm^{-1}$).

In the presence of the enzymatic reaction, LDH@CP-MWCNT (the enzymatic layer for the bioconversion of pyruvate to lactate catalyzed by LDH) was placed on top of the FNR@CP-MWCNT$_{ox}$ electrode, as reported previously with the Rh complex system [24]. The solution containing pyruvate and NAD(P)$^+$ cofactor was fed into the electroenzymatic reactor, where it penetrated through the enzymatic layer (LDH@CP-MWCNT) to reach the electroenzymatic electrode. Here, the regeneration of the cofactor occured, and the regenerated cofactor was coupled with the bioconversion of pyruvate to lactate at the enzymatic layer.

Quantitative analysis of pyruvate bioconversion was performed by HPLC, using the Aminex HPX-87H HPLC column (300 mm × 7.8 mm, Phenomenex) thermostated at 55 °C, and a refractive index detector. The aqueous phase was percolated at 0.2 $mL.min^{-1}$ for 55 min. Pyruvate and lactate were quantified from 200 μL aliquots taken from the reaction mixtures at different intervals.

3. Results and discussion

In this study, the direct electron transfer between FNR and the electrode was investigated. We made the hypothesis that the oxidative treatment of MWCNT that favors the formation of CO-related oxygen groups such as phenol, carbonyl quinones and ether, could improve the affinity of MWCNT towards FNR active site environment in addition to the binding between carbonyl groups of MWCNT and amino groups of FNR. Furthermore, the high electroactive surface of MWCNT layers should make them suitable electrode materials in a flow reactor [27].

3.1. Cyclic voltammetry (CV) experiments

3.1.1. FNR@CP-MWCNT$_{ox}$ electrocatalytic activity towards NADPH regeneration

The electroenzymatic behavior of 20 nmol of FNR immobilized on CP-MWCNT$_{ox}$ was evaluated by cyclic voltammetry at 5 $mV.s^{-1}$ and with hydrogen and solution flow rates of 20 $mL.min^{-1}$.

Without FNR, the electrode did not exhibit any redox activity in the absence (Fig. 1**A curve a**) or in the presence of $NADP^+$ (**Fig. S1**). With 20 nmol drop-casted FNR on the CP-MWCNT$_{ox}$, the redox activity of FNR (Fig. 1**A curve b**) was revealed by the onset of reduction current at −0.45 V vs ref (H_2) and with a reduction vague at −0.67 V vs ref (H_2). Besides, the electrochemical activity of FNR supported by the carbon material did not exhibit an oxidation peak in the reverse scan as reported in previous studies [12,14]. This difference in the electrochemical behavior could be due to the difference in supporting material on which FNR was immobilized. The addition of 2 mM $NADP^+$, Fig. 1**A curve c**, generated a substantial increase in the current at −0.7 V vs ref (H_2) attributed to the electrocatalytic reduction of the cofactor by FNR. Interestingly, increasing the amount of FNR loaded on the electrode surface from 20 nmol to 250 nmol led to an increase in the redox activity with a cathodic current at −0.67 V vs ref (H_2) varying from 5.2 mA to 18.5 mA (**Fig. S2**).

In addition, in order to evaluate the robustness of the FNR@CP-MWCNT$_{ox}$ electrode and its activity, the tested electrode was stored at

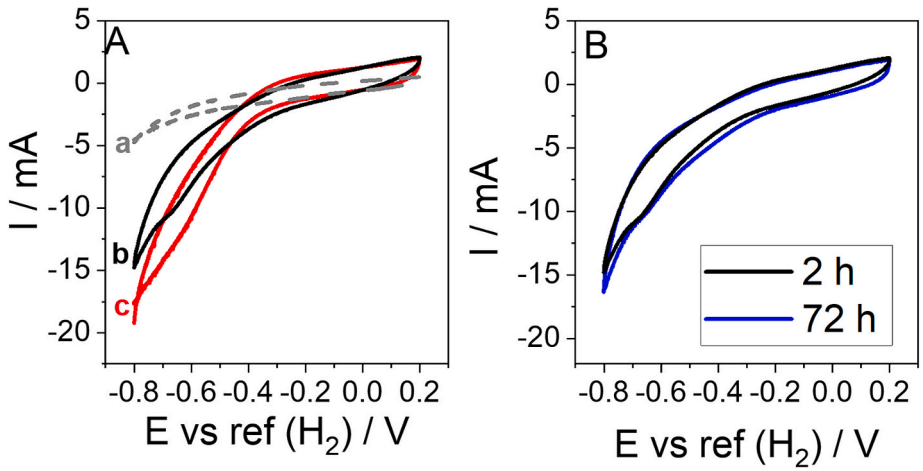


Fig. 1. (A) Cyclic voltammograms recorded at a potential scan rate of 5 mV.s^{-1} in 50 mM TAPS buffer at pH 8 under nitrogen of (a) CP-MWCNT$_{ox}$ and (b,c) FNR@CP-MWCNT$_{ox}$ in the presence of (b) 0 mM and (c) 2 mM NAD(P)$^+$. (B) CV evaluation of the FNR@CP-MWCNT$_{ox}$ electrode activity through cyclic voltammetry in the absence of NADP$^+$ respectively performed 2 h (replicate of Fig. 1A curve b) and 72 h after its preparation. Conditions: 20 nmol of FNR drop casted on CP-MWCNT$_{ox}$, V = 20 mL, H_2 and solution flow rates: 20 mL.min^{-1}.

2 °C in TAPS buffer and was further tested 72 h later. As shown in Fig. 1**B**, the electrode exhibited an electrochemical activity featured by a cathodic current very similar to that recorded two hours after its preparation, showing a maintained activity and stability over time. The high stability is likely due to the high affinity of the positively charged FNR towards the negatively charged surface of oxidized MWCNT at pH 8 [28].

On the other hand, in order to evaluate the effect of MWCNT oxidation on FNR activity and stability, FNR was tested on pristine MWCNT. The catalytic activity of 20 nmol of FNR immobilized on the CP-MWCNT showed the onset of a reduction current at −0.28 V vs ref (H_2) and a cathodic shouldering at −0.37 V vs ref (H_2) showing a current of 0.6 mA. This current was approximately 9 times lower than the one observed on oxidized MWCNT (5.3 mA vs 0.6 mA) (**Fig. S3A curve a**). This reduction peak was approximately 300 mV more positive than the one with MWCNT$_{ox}$. The observed differences in the current response of FNR on pristine and oxidized MWCNT surfaces are significant and seem to be due to the distinct surface properties introduced by oxidation. Oxidative treatment introduces functional groups such as hydroxyl, carboxyl, and carbonyl, which enhance hydrophilicity and can provide stronger interactions between the enzyme and the electrode surface. These functional groups facilitate better enzyme immobilization and more electrocatalytic events. In contrast, on pristine MWCNTs, the absence of such functional groups results in weaker interactions, leading to low catalyst adsorption and poor enzyme orientation.

Then, the effect of the NADP$^+$ cofactor on the electroenzymatic activity of FNR immobilized on pristine MWCNT (FNR@CP-MWCNT) was tested. The addition of 0.5 mM NADP$^+$ revealed an increase in the cathodic current −0.37 V to 1.1 mA (**Fig. S3A curve b**) related to the electroenzymatic activity of FNR towards the regeneration of NADPH. The regeneration of 0.5 mM of NADPH, 2 h after preparation of the FNR@CP-MWCNT electrode, was carried out at an applied electrolysis potential of −0.4 V vs ref (H_2). The current started at approx. −2 mA then decreased strongly after 25 min (**Fig. S3B**). After this period, 56 % of NADPH was regenerated, as measured by UV–visible absorption spectroscopy at 340 nm. Within 60 min of electrolysis, NADPH was totally regenerated with a faradaic efficiency of 74.8 % and with a TTN for FNR near 1000. This faradaic efficiency value can be due to hydrogen evolution reaction (HER) that can be occurring at the same potential. The obtained TTN value is higher than the value obtained with immobilized Rh complex ([Cp*Rh(bpy)Cl]$^+$ covalently immobilized on a carbon paper coated with MWCNT system (300) without the application of an enzymatic reaction [24].

However, the repetition of the electrolysis test at the same electrolysis potential and following the same protocol *e.g.,* 0.5 mM NADP$^+$, 20 mL solution, −0.4 V vs ref, and hydrogen and solution flow rates of 20 mL.min^{-1} after 24 h after the electrode preparation **(Fig. S3C)** showed an electrolysis current that was at least 10 times lower than the one obtained 2 h after the electrode preparation. This strong reduction in the current indicates that FNR@CP-MWCNT has almost lost its activity with time. The average current of the electrolysis was equal to 110 μA during the 160 min-long electrolysis allowing regeneration of only 125 μM NADPH out of the 500 μM NADP$^+$ initially introduced. This clearly shows that the immobilization of FNR on a CP coated with pristine MWCNT cannot lead to a fully active and stable electrode over time and under flow conditions.

Therefore, despite the reduction of NADP$^+$ that occurred at a more negative potential, it was clear that the use of oxidized MWCNT maintained and enhanced the activity of FNR towards NADPH regeneration.

For further tests, a carbon paper modified with a layer of oxidized MWCNT on which FNR was drop-casted was thus selected here as the best one for regeneration of the cofactor.

3.1.2. Does FNR regenerate NADH?

In previous studies, the electroenzymatic regeneration of NADH was normally achieved using NAD$^+$ reductase [29,30], while regeneration of NADPH was catalyzed by FNR [12,13,17]. In the following part, a series of experiments was also carried out for the electrochemical regeneration of NADH instead of NADPH by FNR, although it was reported in the literature that catalysis may be impaired when NAD$^+$ instead of NADP$^+$ is added (i.e., the structure does not contain a phosphate at the 2′-position of the ribose). Based on apparent affinities, K_M for NADP$^+$ lays typically between 8 and 39 μM [17], while it is in the range 4–11 mM for NAD$^+$ [31]) and the selectivity of FNR for NAD$^+$ should be significantly lower than for NADP$^+$.

The electroenzymatic activity of FNR towards NADH regeneration was evaluated through cyclic voltammetry at 5 mV.s^{-1} (Fig. 2**A**). Without NAD$^+$, a cathodic current was observed at −0.67 V vs ref (H_2) referred to the redox behavior of the FNR@CP-MWCNT$_{ox}$ electrode as previously observed (Fig. 1**A**). The addition of 1 mM of NAD$^+$ (Fig. 2**A**) led to an increase in the cathodic current ($|I_{peak}\text{-}I^{+}_{peak)0\ mM\ NAD}|$) at −0.67 V vs ref ($H_2$) of 1.23 ± 0.15 mA. This result accounts for the electrocatalytic activity of FNR@CP-MWCNT$_{ox}$ electrode towards NADH regeneration. Addition of larger amounts of NAD$^+$ resulted in increased cathodic current at −0.67 V vs ref (H_2). For example, the cathodic current at −0.67 V vs ref, Fig. 2**B**, increased from 1.23 ± 0.15

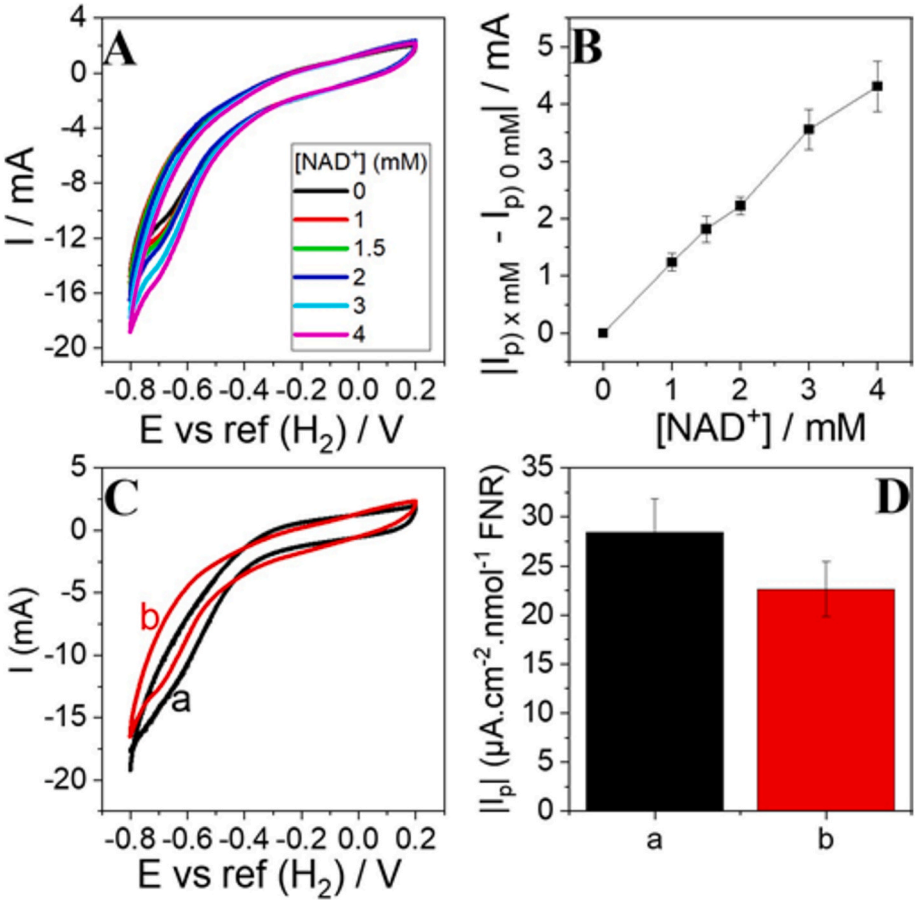


Fig. 2. (A) Cyclic voltammograms of 20 nmol FNR@CP-MWCNT$_{ox}$ electrode recorded at a potential scan rate of 5 mV.s^{-1} in 50 mM TAPS buffer at pH 8 under nitrogen and in the presence of increasing concentrations of NAD^+: 0 mM, 1 mM, 1.5 mM, 2 mM, 3 mM, and 4 mM. (B) Influence of NAD^+ concentration on the cathodic current peak measured by CV for FNR@CP-MWCNT$_{ox}$ electrode at −0.7 V vs ref (H_2). (C, D) Comparison between (C) cyclic voltammograms and (D) current density of FNR@CP-MWCNT$_{ox}$ recorded at −0.7 V after the addition of 2 mM of (a) $NADP^+$ (Duplicate of Fig. 1 **A curve c**) and (b) NAD^+ (Duplicate of Fig. 2**A 2 mM NAD$^+$**). Conditions: V = 20 mL; Hydrogen and solution flow rates: 20 mL.min^{-1}; T = 20 °C.

mA with 1 mM of NAD^+ to 4.30 ± 0.44 mA with 4 mM NAD^+.

The electroenzymatic activity of FNR toward NADH regeneration was further analyzed by examining the difference in currents observed in cyclic voltammetry experiments between the curves in the presence of NAD^+ and in the absence of the NAD^+ cofactor (**Fig. S4C**). These experiments were extracted from CV experiments in the potential range from −0.01 V to −0.8 V vs ref. Two distinct waves were observed in the differential current curves. The first wave, appearing at potentials around −0.4 V with a maximum around −0.67 V vs ref, likely corresponds to the electroenzymatic reduction of NAD^+ catalyzed by FNR. This increase in cathodic current (**Fig. S4D**) is approximately the same as the one obtained from the differential I_p in Fig. 2**B**. The second wave, observed at more negative potentials (−0.71 V), can be attributed to HER. For all concentrations of NAD^+, the current observed in the second wave remained approximately constant.

These findings highlight the complex interplay between the desired electroenzymatic reaction and competing side reactions, such as HER, at the electrode surface. The observed activity further emphasizes the importance of operating conditions to enhance selectivity for NAD^+ reduction and minimize competing reactions.

Besides, the comparison of $NADP^+$ and NAD^+ with respect to the electrochemical behavior of the FNR@CP-MWCNT$_{ox}$ electrode at −0.7 V vs ref (H_2) after the addition of 2 mM of one of the two cofactors (Fig. 2**C),** showed an onset potential of 80 mV approximately more positive obtained with $NADP^+$ (−0.36 V with 2 mM $NADP^+$ vs −0.44 V with 2 mM NAD^+). On the other hand, after addition of 2 mM of NAD^+, FNR@CP-MWCNT$_{ox}$ (Fig. 2**C curve b**) showed a reduction current, at −0.67 V vs ref (H_2), that is 1.83 ± 0.21 mA lower than the one obtained after the addition of 2 mM of $NADP^+$. This small difference (approx. 5.7 ± 2.1 µA.cm^{-2}.nmol^{-1}FNR), as shown in Fig. 2**D,** might be due to the lower affinity of FNR towards NAD^+ than $NADP^+$ [31].

Furthermore, the regeneration of 1 mM NADH was monitored using bulk electrolysis experiments conducted at −0.7 V vs ref (**Fig. S5A**). Before the addition of NAD^+, the current stabilized at approximately −0.4 mA. Upon addition of 1 mM NAD^+, the current increased significantly to −1.3 mA. After 70 min of bulk electrolysis, 1 mM of NADH was successfully regenerated with a faradaic efficiency of 81 %. To confirm the activity of the regenerated cofactor, 100 µM of NADH was tested in an activity assay. This assay was performed using UV–visible absorption spectroscopy in the presence of 50 U of lactate dehydrogenase (LDH) and 1 mM pyruvate (**Fig. S5B**). The absorbance at 340 nm, indicative of NADH concentration, decreased gradually over time, eventually reaching a minimal value after approximately 30 min. This result confirms the regeneration of the active form of NADH (1,4-NADH).

In conclusion, the FNR@CP-MWCNT$_{ox}$ electrode exhibits a high activity not only for NADPH regeneration, but also for NADH regeneration. This allowed us to further explore its application in electroenzymatic biosynthesis while testing the possibility of the application of lower amounts of NAD^+ that can prove the activity of FNR@CP-MWCNT$_{ox}$ towards the regeneration of these low concentrations.

3.2. Application of FNR@CP-MWCNT$_{ox}$ for regenerating NADH in enzymatic reactions

Coupling an enzymatic reaction to the regeneration of NADH by FNR@CP-MWCNT$_{ox}$ can demonstrate the regeneration of the active form of NADH (1,4-NADH). This would be desirable for its application in the synthesis of pure chemicals. In this work, the electroenzymatic regeneration of NADH was coupled to the bioconversion of pyruvate to lactate by LDH to evaluate the efficiency of this in-situ NADH regeneration system.

3.2.1. Parameter optimization for the efficient bioconversion of pyruvate

In this section, two factors of importance have been primarily studied: (i) the molar ratio of the two enzymes employed and (ii) the immobilization procedure of both biocatalysts i.e., either on the same carbon layer as reported in the literature [14,29] or separately, as previously done with Rh complex catalyst [24]. For all experiments, the selected pH for the bioconversion of pyruvate was fixed at 7.6 as a compromise between the optimal pH of FNR (pH = 8) and of LDH (pH = 7.2).

For the first aspect, two simple experiments were carried out to determine how the catalytic performance depends on the ratio of the two enzymes (FNR and LDH) added on the same layer (CP-MWCNT$_{ox}$). Fig. 3 shows the time variations of the current for the reduction of pyruvate to lactate, performed with a 16 cm^2 (FNR + LDH)@CP-MWCNT$_{ox}$ pre-loaded by drop-casting with 20 nmol of FNR and two different amounts of LDH, 20 nmol (Fig. 3 **curve a**) or 4 nmol (Fig. 3 **curve b**). The study was performed in the presence of 5 mM of pyr and 1 mM of NAD$^+$.

At −0.7 V vs ref (H_2) and for an FNR: LDH ratio of 1 (Fig. 3 **curve a**), the current rapidly reached a maximum current of –22 mA related to the catalytic activity of FNR in the presence of 1 mM of NAD$^+$. This current decreased gradually in intensity over time until reaching −15 mA after 9 h. This high current could be due to the HER. Despite the use of 1 mM of NAD$^+$, the bioconversion proceeded very slowly, taking 9 h to reach completion with a faradaic efficiency of only 6 %. Despite the high current of reduction obtained, the high amount of LDH added, corresponding to a ratio at unity on the FNR@CP-MWCNT$_{ox}$, might be a possible cause of higher evolution in hydrogen. The pH of the solution after 9 h of electrolysis was equal to 7.5.

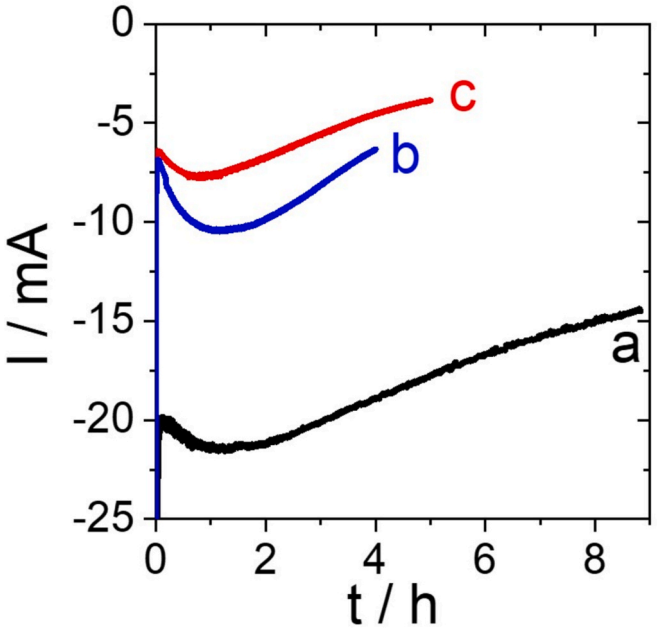


Fig. 3. Effect of the ratio between FNR and LDH and the immobilization of FNR and LDH on the current of a single 16 cm^2 CP-MWCNT layer or on separate layers in batch tests with recirculation, at −0.7 V vs ref. (H_2). (a) (20 nmol FNR + 20 nmol LDH)@CP-MWCNT$_{ox}$, (b) (20 nmol FNR + 4 nmol LDH)@CP-MWCNT$_{ox}$, and (c) 20 nmol FNR@CP-MWCNTox and 4 nmol LDH@CP-MWCNT-LDH (separated layers). Conditions: 1 mM NAD$^+$, 5 mM Pyr, hydrogen and solution flow rates: 20 mL.min^{-1}, V = 30 mL.

Besides, the test with the lower amount of adsorbed LDH on the FNR@CP-MWCNT$_{ox}$ electrode (4 nmol LDH, corresponding to a FNR: LDH ratio of 5) showed an electrolysis current starting at −12 mA (Fig. 3 **curve b**) and decreasing (in absolute value) to −6.5 mA after 4 h. At this time, the bioconversion was complete.

The current monitored here (with FNR:LDH ratio of 5) was approx. 3 times lower than that with identical amounts of FNR and LDH. The faradaic efficiency of pyruvate conversion was accordingly equal to 22 %. In both bioconversion tests, the faradaic efficiency was low compared with that obtained with Rh complex (78 %) [24]. This low value can be due to the negative potential applied for which hydrogen evolution can be observed or to the low density of both catalysts on the 16 cm^2 electrode. Nevertheless, these two experiments indicate that the optimal ratio between FNR and LDH for an efficient bioconversion of pyruvate has to be in the order of 5.

In order to evaluate the effect of the separation of the two biocatalysts on the pyruvate conversion and its faradaic efficiency, the same experiment with an FNR:LDH ratio of 5 was done but each catalyst was drop-casted on a separate CP-MWCNT as illustrated in scheme 1.

In this context, the obtained current of the bioconversion was lower in comparison with the one obtained in the last two experiments (Fig. 3 **curve c**). After a "maximum" value near −7.5 mA, the current decreased gradually with time to reach −3.5 mA after 5 h. The bioconversion was total after 5 h and the faradaic efficiency was equal to 27 %. Pyruvate bioconversion was faster when both enzymes were placed on the same carbon layer, presumably thanks to facilitated transfer of regenerated NADH between catalysts. However, the lower faradaic efficiency (22 %) observed might affect the reactant activity over time owing to the degradation of the cofactor.

In conclusion, in addition to the application of a ratio of 5 between FNR and LDH, the best strategy for optimizing the activity of these two catalysts is to associate them closely while maintaining a negligible separation between them, allowing an efficient cofactor regeneration as well as efficient pyruvate bioconversion.

3.2.2. Towards higher production rate of lactate with a lower amount of NAD$^+$

An important criterion to consider is the production rate of the designed system. For this purpose, it was important to increase the concentration of pyruvate in the initial solution in addition to increasing amounts of enzymes separately immobilized on the CP-MWCNT with the previously optimized FNR:LDH ratio of 5. Another important point to be investigated was the effect of the enzyme amount on the faradaic efficiency of the overall system. Furthermore, the application of low NAD$^+$ concentrations (10 μM) was targeted for the sake of high TTN levels that can compete with values reported in the literature ($TTN_{NAD(P)} > 2000$) [11,29] and for the possible economic viability of the process [11]. In addition, decreasing NAD$^+$ concentrations in the system would validate the fact that FNR can also be used for NADH-coupled reactions in addition to NADPH-coupled reactions.

The bioconversion of 50 mM pyruvate in 60 mL solution containing 10 μM NAD$^+$ – i.e., 3 mmol pyruvate introduced – in the process described in Scheme 1 was carried out at −0.7 V vs ref. (H_2) for 48 h, with the two enzyme carbon-based layers: 50 nmol FNR@CP-MWCNTox and 10 nmol LDH@CP-MWCNT, i.e., 1080 units LDH, and at room temperature in the first set of experiments (Fig. 4**A curve a**).

The bioconversion current was in the order of – 7 mA in the first instants of the run, then gradually decreased (in abs. value) to reach −3.5 mA after 5 h (Fig. 4**A curve a**) whereas 20 % of the pyruvate introduced was converted to lactate within this period (Fig. 4**B curve a**). Then, the (absolute) current increased and reached back (− 7 mA) after

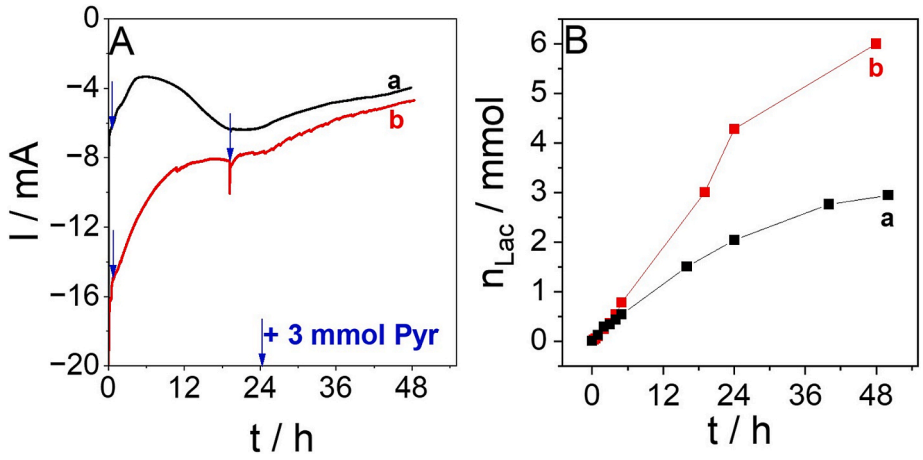


Fig. 4. **(A)** Variation of the current recorded after the addition of pyruvate (blue arrow corresponds to the addition of 3 mmol of pyruvate) at (a) **room temperature** and (b) **35 °C** from 50 mM of pyruvate in 60 mL solution containing 10 μM NAD^+ (and 50 mM TAPS, pH 7.6) in the flow reactor provided with 50 nmol FNR@CP-$MWCNT_{ox}$ electrode and 10 nmol LDH@CP-MWCNT (1080 units) layer. **(B)** Corresponding variations of the amounts of lactate produced at (a) room temperature and (b) 35 °C.

24 h with 2.1 mmol of lactate produced, i.e., with a 70 % conversion extent. Afterward, the current slowly decreased in the second day to reach − 4 mA after 48 h: 2.85 mmol had been produced (Fig. 4**B curve a**).

The current of this bioconversion was in the same order of magnitude that the one with the system with far lower amounts of pyruvate and enzymes (Fig. 3**, curves b and c)**; however, the faradaic efficiency obtained for the bioconversion in the presence of 50 nmol of FNR and 10 nmol of LDH, at 68 %, was more than twice as high than the one observed with 20 nmol FNR and 4 nmol LDH casted separately on CP-MWCNT layers. The low faradaic efficiency obtained previously (Fig. 3) may be attributed to non-optimal amounts of enzymes casted on CP-MWCNT layers with high currents in comparison to the reactant concentrations, thus making the occurrence of HER possible.

TTNs of FNR, NAD^+, and LDH were respectively larger than 5.7×10^4, 4750, and 2.8×10^5. A product rate formation of 74 $nmol.cm^{-2}.h^{-1}.nmol^{-1}$ FNR and a turnover frequency (TOF) of 0.32 s^{-1} were calculated at the end of the 48 h-bioconversion. These values are far higher than the values obtained previously with Rh complex system with 9.5 $nmol.cm^{-2}.h^{-1}.nmol^{-1}$ Rh and a TOF near 0.083 s^{-1} [24].

Since one of the ultimate goal will be to exchange platinum by hydrogenases for hydrogen oxidation and the activity of some O_2-tolerant hydrogenases can be enhanced by temperature [32,33], we investigated the effect of the temperature increase on the activity of the enzyme-bound electrodes (FNR@CP-$MWCNT_{ox}$ & LDH@CP-MWCNT). Moreover, the activity of both FNR and LDH was reported to increase with temperature [34]. For that, a bioconversion reaction was run at 35 °C (following the same conditions of those applied at room temperature) because an FNR homolog from *Chlamydomonas reinhardtii* FNR was reported to become inactive at a temperature higher than 39 °C due to protein unfolding and dissociation of the FAD cofactor [35].

The 48 h-long tests consisted in adding 6 mmol of pyruvate in two steps at t = 0 (3 mmol Pyr) and at t = 19 h (3 mmol Pyr) in the flow reactor operating at 35 °C. The total volume of the solution after the second addition of Pyr is 60 mL. The current recorded starting at approx. −15 mA decreased to −8.5 mA after 18 h (Fig. 4**A curve b**), whereas the first pyruvate charge introduced, 3 mmol, was nearly totally converted to lactate (Fig. 4**B curve b**). On average, the current recorded here (Fig. 4**A curve b**) was nearly twice as large than that recorded at ambient temperature (Fig. 4**A curve a**).

The addition of 3 mmol of pyruvate after 19 h resulted in a small pulse in the current, which then decreased until the end of the run (Fig. 4**A curve b**). After this 48 h-run, a total bioconversion of pyruvate was obtained resulting in the formation of 6 mmol of lactate (Fig. 4**B curve b**). The overall faradaic efficiency reached 88 %, to be compared with the 68 % at ambient temperature (Table 1 **experiments 1 and 2**).

In conclusion, this result illustrates that the enzymatic activities increased with temperature, enhancing the rate of cofactor regeneration and pyruvate bioconversion to lactate. The increased faradaic efficiency could be due to a relatively lower contribution of HER at 35 °C versus room temperature, despite that HER can also increase with temperature. Overall, the increased enzymatic activities appeared to be beneficial for the selectivity of the electrochemical reaction. In comparison with the experiment at room temperature (Table 1 **experiment 1**), the production rate of lactate (156 $nmol.h^{-1}.cm^{-2}.nmol^{-1}$ FNR, Table 1 **experiment 2**), was doubled at 35 °C, in addition to the larger faradaic efficiency.

With the increase in the production rate, TTNs for FNR, NAD^+, and LDH attained very high values at 1.2×10^5, 10^4, and 6×10^5 respectively. TTN for the cofactor is more than 2 times higher than the one obtained at room temperature. TTN obtained for FNR and NAD^+ are – to the best of our knowledge – the highest values among those reported in the literature [11,12,29].

Having a system that confirmed its activity towards the bioconversion of pyruvate with a high faradaic efficiency, it was important to test a possible scaling up by using higher amounts of pyruvate and higher amounts of enzymes loaded on both electrodes surfaces. This has been done in the same reactor, with larger enzyme amounts and a larger volume of solution to be treated.

Following the optimization applied before *e.g.,* FNR: LDH = 5, the immobilization of enzymes on separated supports with a minimized distance between them, at T = 35 °C, and the electrolysis potential (−0.7 V vs ref (H_2)), the volume of solution was increased ten times, with an initial volume of 500 mL to which 100 mL pyruvate (0.5 M) solution was added in several steps throughout the 6-day run, for a final volume of 600 mL. Pyruvate addition was as follows: 15 mmol – 30 mL at t = 0h, 15 mmol – 30 mL at t = 24 h, 10 mmol – 20 mL at t = 43 h, 5 mmol – 10 mL at t = 91 h, and 5 mmol – 10 mL at t = 120 h. The amount of drop-casted enzymes on the 16 cm^2 electroenzymatic electrode and the 16 cm^2 enzymatic layer was 5-fold increased (250 nmol FNR@CP-$MWCNT_{ox}$ and 50 nmol (5400 units) LDH@CP-MWCNT, still in the presence of 10 μM NAD^+.

The first addition of 15 mmol pyruvate resulted in a rapid increase in the current from –22.5 mA to −37.5 mA (**Fig. S6A**). Then, the current sharply decreased as the reactant was depleted: 10.8 mmol of lactate (20.3 mM) were produced within the first 24 h (**Fig. S6B**) with a faradaic efficiency of 93 %. The corresponding production rate was equal to 113 $nmol.h^{-1}.cm^{-2}.nmol^{-1}$ FNR. This value is in the same order of

Table 1
Effect of the temperature and the process scaling up on pyruvate bioconversion kinetics and on the current efficiency. (*) Faradaic efficiency is for lactate production.

Experiment	T (°C)	Pyruvate added (mmol)	Lactate produced (mmol)	t (h)	Production rate ($nmol.h^{-1}.cm^{-2}.nmol^{-1}FNR$)	TTN_{NAD}	Faradaic efficiency* (%)
1	20	3	2.85	48	125 ± 30	4750	68
2	35	6	6	48	158 ± 36	10,845	88
3	35	50	45.5	120	113 ± 20 (*After 24 h*)	9200	81

magnitude as the value reported before with the lower volume and catalysts amounts (Fig. 4**B curve b;** Table 1 **experiment 2**). The sustained additions of pyruvate showed a continuous increase in the bioconversion of pyruvate within the first 5 days. After this time, the bioconversion stabilized at 45.5 mmol of Lac (76 mM) with a faradaic efficiency of 81 % at 120 h (**Fig. S6B;** Table 1 **experiment 3**) and TTNs for FNR, NAD^+, and LDH reached 1.82 x 10^5, 9200, and 9.1 × 10^5, respectively. The TTN for FNR and LDH were higher than those obtained at smaller scale, whereas the TTN for NAD^+ (Table 1 **experiment 2 and 3**) was in the same order of magnitude.

In order to investigate the cause of the conversion stop after 5 days (120 h), the redox response of FNR after these 6 days was evaluated by cyclic voltammetry at pH 8 (**Fig. S7**). The two voltammograms obtained 2 h after the electrode preparation (**Fig. S7 curve a**) and 6 days of electrolysis (**Fig. S7 curve b**) exhibit similar profiles and the cathodic current at −0.7 V vs ref (H_2) was almost the same as that measured 2 h after the electrode preparation.

Besides, we noticed that the pH of the solution decreased from 7.6 to 6.2 in the course of the 6-day run. Whereas LDH should remain active at pH around 7.0, FNR is known to require higher pH: therefore, the stop in the conversion could be due to the decay of FNR activity with the decrease in pH or to the need of a buffer exchange.

Despite the interruption of the bioconversion after 6 days, scaling-up the reactor was shown possible with larger amounts of enzymes loaded on the carbon layer surfaces.

4. Conclusion

In summary, we have demonstrated in this work a full potential of an electroenzymatic flow reactor in which FNR was immobilized on carbon paper coated with oxidized MWCNT for the coupling of an efficient NAD(P)H regeneration to the oxidation of hydrogen. The prepared FNR@CP-$MWCNT_{ox}$ electrode retains activity over time, at least 6 days under continuous electrolysis and flow conditions.

Interestingly, in the set of experiments presented, FNR shows its activity not only towards the NADPH cofactor regeneration, but also towards the regeneration of NADH cofactor. The electroenzymatic regeneration of NADH by FNR has been coupled to the bioconversion of pyruvate and showed that the active form of NADH has been regenerated (1,4-NADH).

In this work, experimental techniques, namely FNR immobilization on oxidized MWCNT, immobilization of FNR and LDH on stacked but distinct CP-MWCNT layers, as well as operating conditions *e.g.*, temperature at 35 °C and FNR: LDH ratio near 5, have been largely improved. Under optimal conditions, the bioconversion system of pyruvate to lactate conducted with low amounts of NAD^+ (10 μM) has scored high levels of TTNs for FNR, NAD^+, and LDH with 1.2 x 10^5, 10^4, and 6 x 10^5 respectively with a faradaic efficiency of 88 % and a productivity of 156 $nmol.h^{-1}.cm^{-2}.nmol^{-1}$ FNR. In addition, the scaling up of the system from 60 mL to 600 mL proved to be successful with a preserved high productivity level (113 $nmol.h^{-1}.cm^{-2}.nmol^{-1}$ FNR), high levels of TTNs for FNR, NAD^+, and LDH of 1.82 x 10^5, 9200, and 9.2 x 10^5 respectively, and a faradaic efficiency of 83 %. With a better control of the system, results in this work suggest that the linear scaling of solution volume might be possible with the application of cascades of electrodes of both FNR@CP-$MWCNT_{ox}$ and LDH@CP-MWCNT supported with high amounts of enzymes.

The next logical step, as previously outlined, could be the transition towards a fully electroenzymatic reactor that couples hydrogen oxidation, catalyzed by hydrogenases, to the reduction of $NAD(P)^+$ by FNR. This strategy holds considerable promise, especially from a green chemistry standpoint. By integrating such a system, we could achieve continuous and efficient regeneration of NAD(P)H, which is crucial for biosynthetic processes. Moreover, it would minimize the reliance on platinum catalysts, offering both environmental and economic benefits. This approach would not only align with sustainability goals but would also enhance the feasibility of large-scale biochemical synthesis. Such advancements in electroenzymatic systems could redefine how we approach chemical production, making it more efficient and environmentally friendly.

CRediT authorship contribution statement

Wassim El Housseini: Writing – review & editing, Writing – original draft, Methodology, Investigation. **François Lapicque:** Writing – review & editing, Validation, Supervision, Funding acquisition, Conceptualization. **Alain Walcarius:** Writing – review & editing. **Elisabeth Lojou:** Writing – review & editing, Supervision, Funding acquisition. **Nicolas Rouhier:** Writing – review & editing, Resources. **Mathieu Etienne:** Writing – review & editing, Supervision, Project administration, Funding acquisition, Conceptualization.

Declaration of competing interest

The authors declare that they have no known competing financial interests or personal relationships that could have appeared to influence the work reported in this paper.

Acknowledgements

We gratefully acknowledge CNRS for funding of the project NADP/H_2.

Appendix A. Supplementary data

Supplementary data to this article can be found online at https://doi.org/10.1016/j.bioelechem.2025.108919.

Data availability

Data will be made available on request.

References

[1] S. Broussy, R.W. Cheloha, D.B. Berkowitz, Org. Lett. 11 (2009) 305–308.
[2] N.J. Turner, Nat. Chem. Biol. 5 (2009) 567–573.
[3] H.A. Reeve, P.A. Ash, H. Park, A. Huang, M. Posidias, C. Tomlinson, O. Lenz, K. A. Vincent, Biochem. J. 474 (2017) 215–230.
[4] L. Zhang, M. Etienne, N. Vilà, T.X.H. Le, G.-W. Kohring, A. Walcarius, ChemCatChem 10 (2018) 4067–4073.
[5] C.F. Megarity, B. Siritanaratkul, B. Cheng, G. Morello, L. Wan, A.J. Sills, R.S. Heath, N.J. Turner, F.A. Armstrong, ChemCatChem 11 (2019) 5662–5670.
[6] W. Hummel, M. -r kula,, Eur. J. Biochem. 184 (1989) 1–13.
[7] H.K. Chenault, G.M. Whitesides, Appl. Biochem. Biotechnol. 14 (1987) 147–197.

[8] L. Gorton, E. Domínguez. Encycl. Electrochem, Wiley, 2007, https://doi.org/10.1002/9783527610426.bard090004.
[9] E. Steckhan, S. Herrmann, R. Ruppert, E. Dietz, M. Frede, E. Spika, Organometallics 10 (1991) 1568–1577.
[10] A. Walcarius, R. Nasraoui, Z. Wang, F. Qu, V. Urbanova, M. Etienne, M. Göllü, A. S. Demir, J. Gajdzik, R. Hempelmann, Bioelectrochemistry 82 (2011) 46–54.
[11] B. Cheng, L. Wan, F.A. Armstrong, ChemElectroChem 7 (2020) 4672–4678.
[12] L. Castañeda-Losada, D. Adam, N. Paczia, D. Buesen, F. Steffler, V. Sieber, T.J. Erb, M. Richter, N. Plumeré, Angew. Chemie - Int. Ed. 60 (2021) 21056–21061.
[13] X. Wang, T. Saba, H.H.P. Yiu, R.F. Howe, J.A. Anderson, J. Shi, Chem 2 (2017) 621–654.
[14] C.F. Megarity, B. Siritanaratkul, R.S. Heath, L. Wan, G. Morello, S.R. FitzPatrick, R. L. Booth, A.J. Sills, A.W. Robertson, J.H. Warner, N.J. Turner, F.A. Armstrong, Angew. Chemie - Int. Ed. 58 (2019) 4948–4952.
[15] H. Chen, T. Tang, C.A. Malapit, Y.S. Lee, M.B. Prater, N.S. Weliwatte, S.D. Minteer, J. Am. Chem. Soc. 144 (2022) 4047–4056.
[16] I. Mazurenko, V.P. Hitaishi, E. Lojou, Curr. Opin. Electrochem. 2 (2020) 113–121, https://doi.org/10.1016/j.coelec.2019.11.004.
[17] B. Siritanaratkul, C.F. Megarity, T.G. Roberts, T.O.M. Samuels, M. Winkler, J. H. Warner, T. Happe, F.A. Armstrong, Chem. Sci. 8 (2017) 4579–4586.
[18] H. Chen, O. Simoska, K. Lim, M. Grattieri, M. Yuan, F. Dong, Y.S. Lee, K. Beaver, S. Weliwatte, E.M. Gaffney, Chem. Rev. 120 (2020) 12903–12993.
[19] M. Yuan, S.D. Minteer, Curr. Opin. Electrochem. 15 (2019) 1–6.
[20] H.A. Reeve, L. Lauterbach, O. Lenz, K.A. Vincent, ChemCatChem 7 (2015) 3480–3487.
[21] R.W. Coughlin, M. Aizawa, B.F. Alexander, M. Charles, Biotechnol. Bioeng. 17 (1975) 515–526.
[22] S.K. Yoon, E.R. Choban, C. Kane, T. Tzedakis, P.J.A. Kenis, J. Am. Chem. Soc. 127 (2005) 10466–10467.
[23] D. Holtmann, T. Krieg, L. Getrey, J. Schrader, Catal. Commun. 51 (2014) 82–85.
[24] W. El Housseini, F. Lapicque, S. Pontvianne, N. Vilà, I. Mazurenko, A. Walcarius, M. Etienne, ChemElectroChem 9 (2022) e202200463.
[25] P. Schenk, S. Baumann, R. Mattes, H. Steinbiss, Biotechniques 200 (1995) 196–200.
[26] I.A. Safo, F. Liu, K. Xie, W. Xia, Mater. Chem. Phys. 214 (2018) 472–481.
[27] R.L. McCreery, Chem. Rev. 108 (2008) 2646–2687.
[28] G. Kurisu, M. Kusunoki, E. Katoh, T. Yamazaki, K. Teshima, Y. Onda, Y. Kimata-Ariga, T. Hase, Nat. Struct. Biol. 8 (2001) 117–121.
[29] X. Zhao, S.E. Cleary, C. Zor, N. Grobert, H.A. Reeve, K.A. Vincent, Chem. Sci. 12 (2021) 8105–8114.
[30] J. Cracknell, K. Vincent, F. Armstrong, Chem. Rev. 108 (2008) 2439–2461.
[31] M. Shin, Methods Enzymol 23 (1971) 440–447.
[32] K. Monsalve, I. Mazurenko, C. Gutierrez-Sanchez, M. Ilbert, P. Infossi, S. Frielingsdorf, M.T. Giudici-Orticoni, O. Lenz, E. Lojou, ChemElectroChem 3 (2016) 2179–2188.
[33] I. Mazurenko, R. Clément, D. Byrne-Kodjabachian, A. de Poulpiquet, S. Tsujimura, E. Lojou, J. Electroanal. Chem. 812 (2018) 221–226.
[34] S.N. Buhl, K.Y. Jackson, R.E. Vanderlinde, Clin. Chim. Acta 80 (1977) 265–270.
[35] B. Xie, S. Bishop, D. Stessman, D. Wright, M.H. Spalding, L. J. Halverson (2013) 1544–1555.